Simultaneous TE Analysis of 19 Heliconiine Butterflies Yields Novel Insights into Rapid TE-Based Genome Diversification and Multiple SINE Births and Deaths

David A. Ray[1,*], Jenna R. Grimshaw[1], Michaela K. Halsey[1], Jennifer M. Korstian[1], Austin B. Osmanski[1], Kevin A. M. Sullivan[1], Kristen A. Wolf[1], Harsith Reddy[1], Nicole Foley[1,7], Richard D. Stevens[2], Binyamin A. Knisbacher[3,8], Orr Levy[4], Brian Counterman[5], Nathaniel B. Edelman[6], and James Mallet[6]

[1]Department of Biological Science, Texas Tech University

[2]Department of Natural Resources Management, Texas Tech University

[3]The Mina and Everard Goodman Faculty of Life Sciences, Bar-Ilan University, Ramat Gan, Israel

[4]Department of Physics, Bar-Ilan University, Ramat Gan, Israel

[5]Department of Biological Sciences, Mississippi State University

[6]Department of Organismic and Evolutionary Biology, Harvard University

[7]Present address: Department of Veterinary Integrative Biosciences, College of Veterinary Medicine, Texas A&M University, College Station, TX

[8]Present address: Broad Institute of MIT and Harvard, Cambridge, MA

*Corresponding author: E-mail: david.4.ray@gmail.com.

Accepted: June 11, 2019

Abstract

Transposable elements (TEs) play major roles in the evolution of genome structure and function. However, because of their repetitive nature, they are difficult to annotate and discovering the specific roles they may play in a lineage can be a daunting task. Heliconiine butterflies are models for the study of multiple evolutionary processes including phenotype evolution and hybridization. We attempted to determine how TEs may play a role in the diversification of genomes within this clade by performing a detailed examination of TE content and accumulation in 19 species whose genomes were recently sequenced. We found that TE content has diverged substantially and rapidly in the time since several subclades shared a common ancestor with each lineage harboring a unique TE repertoire. Several novel SINE lineages have been established that are restricted to a subset of species. Furthermore, the previously described SINE, Metulj, appears to have gone extinct in two subclades while expanding to significant numbers in others. This diversity in TE content and activity has the potential to impact how heliconiine butterflies continue to evolve and diverge.

Key words: evolution, transposable elements, butterflies.

Introduction

Transposable elements (TEs) have been described as "drivers of genome evolution" (Kazazian 2004). Indeed, TEs are major contributors to processes that influence genomic change (Kidwell and Lisch 1997). TEs mediate small-scale changes but also influence large-scale structural changes including deletions, translocations, duplications, ectopic recombination and are intimately associated with the evolution of genome size in some lineages (Lim and Simmons 1994; Gray 2000; Hedges and Deininger 2007; Carbone et al. 2014; Grabundzija et al. 2016; Kapusta et al. 2017). Transposition is an efficient mechanism for generating widespread genetic diversity that evolutionary processes may build on, leading to phenotypic and taxonomic diversity. While structural changes induced by the insertion of hundreds or thousands of 200–10,000 bp units at a time are likely important to evolutionary processes, it has also been argued that by contributing multiple copies of ready-to-use regulatory motifs, transposons also induce more subtle but also more significant (in the long run) regulatory innovation (Rebollo et al. 2010, 2012; Ellison and Bachtrog 2013; Jacques et al. 2013; Sundaram et al. 2014;

Chuong et al. 2016, 2017; Mita and Boeke 2016; Sundaram et al. 2017; Trizzino et al. 2017).

The idea that by generating genomic diversity TEs play a significant role in adaptive change is not new. On the contrary, the discoverer of TEs herself, Barbara McClintock, proposed that TEs may act as a mechanism for the genome to respond to stress in an adaptive manner (McClintock 1956, 1984). More recently, Oliver and Greene (2011, 2012) proposed the TE Thrust Hypothesis, suggesting that TEs enhance evolutionary potential by introducing variation in the genomes they occupy. In a related hypothesis, Zeh et al. (2009) suggested reduced epigenetic suppression of TEs when organisms are under stress, thereby increasing their activity and their impact on genome structure. This is referred to as the Epi-Transposon Hypothesis. Other authors have offered similar and/or related ideas, in every case linking transposon activity to adaptation (Jurka et al. 2012; Koonin 2016a, 2016b). Alternatively, others have suggested that TE distributions and diversity result mainly from population genetic processes (Jurka et al. 2011).

While all of these ideas represent significant advances in our understanding of TE-genome interactions, several limitations have restricted the scope of research on the relationship between TEs and diversification, preventing tests of these major hypotheses and generalization across taxa. First, the comparisons undertaken thus far involve relatively deep divergences that make understanding the changes that occur at lower taxonomic levels difficult to tease apart. Second, cost effective approaches to densely sample divergent clades have only become available recently, limiting prior comparisons to such deep divergences in an effort to maximize observable differences. Third, a mechanistic understanding of TE action has been confined to lab models and their cell lines, limiting research into the emergence, and control of phenotypic traits. However, recent advances have created opportunities to move past these barriers. Primarily, cost reductions and advances in sequencing technologies and genome analysis have allowed us to examine larger and larger numbers of whole genomes, including whole genome comparisons among relatively closely related species (Lamichhaney et al. 2015; Nater et al. 2015). A narrowed focus has the potential to inform the scientific community of the influences TEs may have at the early stages of taxonomic divergence.

Butterflies of the genus *Heliconius* and related genera are models for the study of several evolutionary processes from hybridization to the evolution of Müllerian mimicry (Heliconius 2012). They have experienced multiple recent bursts of speciation and represent an adaptive radiation that is ripe for study at the genome level (Supple et al. 2013, 2014; Kozak et al. 2015; Arias et al. 2017). These characteristics create an excellent opportunity to examine patterns of TE evolution in a rapidly diversifying clade, allowing us to ask questions about how the TEs themselves evolve as species diverge from one another.

TEs from *Heliconius* were first described as part of the first *Heliconius melpomene* genome project (Heliconius 2012) and examined in detail by Lavoie et al. (2013). In that work, the TE landscape was revealed to be exceptionally diverse with large numbers of active LINEs (Long INterspersed Elements) and large genome proportions derived from SINEs (Short INterspersed Elements) and rolling circle (RC) transposons (Helitrons). Further, the genome was shown to be labile, especially with regard to larger TEs, which appear to be removed regularly via nonhomologous recombination. This is in line with recent hypotheses related to genome evolution and TE content, and in particular, the accordion model of genome evolution, in which some DNA is contributed while other DNA is jettisoned over evolutionary time (Kapusta et al. 2017).

Recently, de novo genome assemblies were generated for multiple representatives of this clade providing us with an opportunity to examine the evolution of TEs in detail across 20 heliconiine species (Edelman et al., 2018). We performed de novo TE annotations on 19 of these genomes and compared the TE landscapes across the heliconiine tree, revealing patterns of TE evolution not yet seen at this fine a scale. We see that differential TE accumulation can be established rapidly across lineages and that particular families and subfamilies establish themselves differentially in independent lineages in relatively short periods of time.

This detailed examination of TE evolution in closely related species lays the groundwork for additional analysis of TEs as members of genomic communities that evolve in ways similar to natural communities in ecosystems. It also opens the door to examining genomic factors that may influence the relative success of TEs in each genome as they diverge from one another.

Materials and Methods

TE Discovery and Classification

De novo TE discovery was implemented using a combination of RepeatMasker (Smit et al. 2013–2015), RepeatModeler (Smit and Hubley 2008–2015), and manual annotation as described in Platt et al. (2016) with some modification. Briefly, each genome assembly was sorted by scaffold length and the top ~200 Mb (the minimum value in the range of genome sizes) were used as the base for our analysis. Each genome fragment was then subjected to a RepeatModeler analysis and a de novo repeat library was generated. Each genome fragment was then masked using its de novo library. RepeatMasker output was processed using the calcDivergenceFromAlign.pl RepeatMasker utility to calculate K2P distance from the corresponding consensus for each insertion.

Because our primary interest is in lineage-specific insertion patterns, we sorted insertions by K2P distance and selected only insertions that were likely to be recent. K2P distance

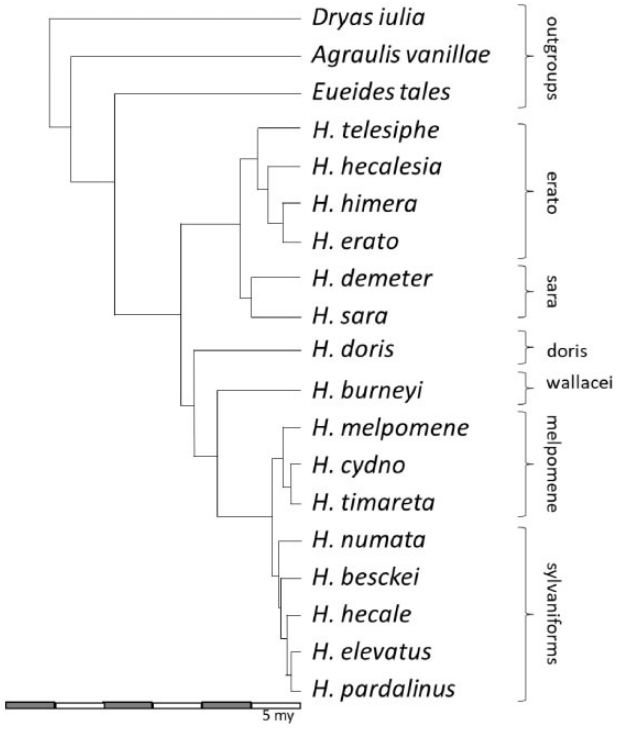

Fig. 1.—Phylogeny of the taxa examined, modified from Kozak et al. (2015). Subclade memberships are identified to the right of the tree.

cutoff values were determined using information from the phylogeny of Kozak et al. (2015). For example, several subgroups are evident from the phylogeny in figure 1. Three species form a relatively deeply diverged set of outgroup taxa, *A. vanillae*, *D. iulia*, and *E. tales*. Because of the longer branch lengths, these species are likely to harbor older but still lineage-specific insertions compared with species in the more recently diversified clades. We therefore examined any insertions with divergences <0.2 in the outgroups ($\sim$13.2 Myr, assuming a neutral mutation rate of 1.9×10^{-9} substitutions/site/generation and 4 generations/year). Similarly, we used reduced cutoffs for members of the other three groups (i.e., divergences <0.1 [$\sim$6.6 Myr] for members of the doris and wallacei clades and <0.05 [$\sim$3.3 Myr] for members of the erato, sara, melpomene, and sylvaniform clades).

Manual validation of putative repeats discovered by RepeatModeler was performed as described in Platt et al. (2016) by using them as queries against a combined "pseudogenome" consisting of a concatenation of each 200 Mb fragment draft with BLASTn v2.2.27 (Altschul et al. 1990). Repeats with fewer than ten hits were discarded from downstream analyses. For all remaining queries, the top hits (up to 40) were extracted with at least 500 bases of flanking sequence and aligned with the query using MUSCLE v3.8.1551 (Edgar 2004). Majority rule consensus sequences were generated in BioEdit v7.2.5 (Hall 1999) and manually edited to confirm gaps and ambiguous bases. 5′ and 3′ ends were examined for single copy DNA, indicating element boundaries. If no single copy DNA was identifiable, the new consensus was subjected to new iterations until boundaries were detected. After each round, new consensus sequences were subjected to a consolidation check using cd-hit-est (Li and Godzik 2006) to identify consensus sequences that could be combined. Criteria for collapsing two or more consensus sequences to a single consensus were 90% identity over at least 90% of their total length.

Broad categories of TE classifications for new TE consensus sequences (i.e., DNA transposons, RC transposons, LINEs, SINEs, LTR elements, and unknown) were determined using a combination of BLAST searches of the NCBI database and CENSOR searches of Repbase (Jurka et al. 2005; Kohany et al. 2006). If hits were obtained and the two resources agreed on the TE classification, we used that classification. However, many novel TEs were not present in either database. We therefore used structural criteria as follows: for DNA transposons, only elements with visible terminal inverted repeats were named as such. For RC transposons we required elements to have an identifiable ACTAG at one end. LTR retrotransposons were required to have recognizable hallmarks such as TG, TGT, or TGTT at their 5′ and the inverse at the 3′ ends. Potential LINE elements were required to have repetitive tails, be longer than 500 bp, and/or have homology to known LINE ORFs. Putative novel SINEs were inspected for a repetitive tail and A and B boxes. Because of the complexity of SINE evolution, putative SINEs were also analyzed uniquely as described below. While sequences in the unknown category could be TEs, they formed only a very small fraction of the total putative TE sequence, and they could also represent segmental duplications or other non-TE species. Our interest was in the TE dynamics in these genomes, thus, these were ignored in most downstream analysis. All other categories were checked for high similarity to known TEs and to one another using a final combined run of cd-hit-est using the same criteria as previous.

SINEs

SINE evolution is complex and identifying subfamily structure is a difficult problem, primarily due to the high number of insertions typical of a genome. Initial analysis suggested three SINE families in these genomes. The first is the previously described Metulj family. The second is a novel family that appears to be derived from the fusion of Zenon LINE 3′ tails with a 5′ head of unknown origin, which we call ZenoSINE. A small subfamily distinct from the main ZenoSINE family was identified in and restricted to the *A. vanillae* genome *A. vanillae* is commonly known as the Gulf Fritillary. Thus, we dubbed this subfamily "Fritillar." Finally, a third family that is derived from R1 elements is restricted to *D. iulia*. One common moniker for this species is "flambeau" and we suggest the same name, Flambeau, for this family of SINEs.

Metulj SINEs were far more numerous and widespread than their ZenoSINE cousins (discussed below), and therefore represented a more difficult analytical problem. A recently developed network-based method for subfamily (aka community) detection was used to identify Metulj subfamilies (Levy et al. 2017). Briefly, similarity networks were constructed by pairwise-aligning Metulj elements >240 nucleotides long ($n = 498{,}141$) from all 19 butterfly genomes using BLAST. Further preprocessing was performed to prevent possible biases caused by sequence length and shared poly(A/T) tails that may confound community detection. For this step, previously identified Metulj consensus sequences were aligned using MUSCLE and 5′ and 3′ overhangs were manually trimmed using Bioedit. Genomic Metulj sequences were aligned to these trimmed consensus sequences using BLAST+ to identify corresponding regions (parameters: *-strand plus -max_target_seqs 3 -num_threads 20 -word_size 4 -evalue 1e-2 -dust no -soft_masking false*). Minimum start and maximum end positions define the region for further analysis per sequence and were length-filtered for ≥235 nucleotides. The 420,689 sequences retained were analyzed for subfamily detection: the sequences were pairwise aligned using BLAST (version 2.7.1+; BLASTn command was used with nondefault parameters: *-strand plus -dust no -max_target_seqs 50 -word_size 8 -soft_masking false*). Bornholdt community detection (Reichardt and Bornholdt 2006) was applied using *gamma = 59*. Consensus sequences were computed using MUSCLE with 30 randomly selected sequences per community (with maximum of two iterations). To further refine subfamily definitions, communities with identical consensus sequences were merged (such pairs were identified using BLAST requiring 100% identity and 95% query coverage). Consensus sequences were computed per subfamily and were used to refine the subfamily annotation, resulting in a final set of 2,493 subfamilies (supplementary file 2, Supplementary Material online). This set was further grouped into 147 clusters to simplify downstream analyses using cd-hit-est. Clustering criterion was 95% identity, comparing the entire length of the SINEs.

LINEs

Previous analyses (Lavoie et al. 2013) suggest that longer TEs are more likely to be fragmented by nonhomologous recombination. As a result, we focused on the LINE ORF to increase the potential for comparable data. A special effort was made to identify full- or near full-length ORFs for each clade. First, we identified all known LINE elements from the *H. melpomene* genome in RepBase. These were combined with any LINEs identified in our de novo analysis after removing possible duplicates. All remaining elements were filtered, retaining any with intact ORFs of at least 2 kb, starting with methionine, and with clearly identifiable start and stop codons using "getorf" from the EMBOSS package (Rice et al. 2000).

To identify subfamily structure of LINEs, phylogenetic analysis of these ORFs was accomplished by masking each genome with the resulting library and retaining any hits of 1.5 kb or longer. Generally, extracted hits were aligned using MUSCLE and subjected to a neighbor-joining (NJ) analysis (described below). However, large numbers of hits impeded efficient alignment in some cases due to memory limitations. To work around this problem, we reduced the number of hits by randomly selecting smaller numbers of sequences from the pool and realigning until successful. In some of these cases, there was a lack of overlapping sites that impeded the NJ analysis. In these cases, we extended our filter to include hits that were at least 2 kb, producing the needed overlapping regions.

Each set of aligned ORFs was subjected to NJ analysis to identify any apparent structure. NJ analyses were accomplished based on the maximum composite likelihood parameters in MEGA7 (Kumar et al. 2016) with pairwise deletion of ambiguous positions and 500 bootstrap replicates. Trees were examined visually and clearly delineated clades with high bootstrap support were labeled as subfamilies using letter designations (Sookdeo et al. 2018; supplementary file 2 and supplementary fig. 13, Supplementary Material online). For example, examination of the RTE-4_Hmel tree yielded four subfamilies, RTE-4_Hmel_A-D (supplementary fig. 13, Supplementary Material online).

To estimate genetic distances among members of each subfamily, we used a combination of tools via a custom script that would first align the hits identified for each subfamily using MUSCLE. The script would then invoke trimal (-gt 0.6 -cons 60 -fasta) to trim the alignment (Capella-Gutierrez et al. 2009) and use "cons" from the EMBOSS package to generate a consensus sequences (-plurality 3 -identity 3). We then used MEGA7 to calculate mean divergence from the consensus, mean divergence among subfamily members, and divergence ranges (supplementary file 3, Supplementary Material online). This and all other custom scripts are available upon request.

Recent versus Ancient Taxonomic Distributions

To determine taxonomic distributions for each class, family, and subfamily, we used RepeatMasker and custom python scripts to generate proportion tables as follows. RepeatMasker was used to identify insertions in each of the 19 genomes, this time using the entire genome drafts. Hits with divergences <0.05 from their respective consensus sequences were considered "recent" and >0.05 as "old." For each TE (separated by names, class, or family, depending on the level of analysis), total base coverage was calculated and divided by the total genome size to give a proportion.

To illustrate differences among *Heliconius* spp. In terms of TE composition, we imposed a principal components (PC) analysis on a species-by-element matrix each for DNA transposons, LTR retrotransposons, SINE's and LINE's. To illustrate

similarities and differences among Heliconiini, we displayed their positions based on the first two PCs. Species that are proximate in this 2D space have more similar TE composition than species that are more distant. To illustrate how species differed based on their TE composition, we displayed the correlation of each individual element type (e.g., those with unique names) with the first and second PC.

SINE/LINE Partnerships

SINEs and LINEs have a host–parasite relationship, in which SINEs will hijack the enzymatic machinery encoded by their partner LINE to mobilize (Kajikawa and Okada 2002; Roy-Engel et al. 2002; Dewannieux et al. 2003). Such partnerships are often defined by a shared 3′ tail (Ohshima and Okada 2005). We examined the 3′ ~100 bp of each SINE and queried the 3′ ends of all LINEs in our new TE database to determine the likely LINE partner for each.

The 3′ tails of Metulj elements exhibited substantial complexity, with a variety of structures including poly-A tracts, poly-T tracts, repeated ATTTA motifs, and repeated GATG motifs, among several others. Based on previous work, we suspected that differences in the tail may influence relative success in retrotransposition (Dewannieux and Heidmann 2005; Ohshima and Okada 2005). To investigate how tail structure evolved, we extracted 100 random full-length Metulj insertions from each taxon. Each set of extracts was aligned to representative consensus sequences. This was repeated ten times for each taxon. The 3′ ends of each alignment were degapped starting where the tail begins and the ratios of each pair of nucleotides was identified and plotted after log-transformation. This was conducted separately for "old" and "young" SINEs.

To determine if either Metulj or ZenoSINE accumulation patterns were correlated with any LINE elements, Pearson correlation coefficients based on proportion of each genome occupied were visualized using the "corrplot" package in R and RStudio v1.0.143.

TE Origination Rates

To estimate approximate rates that lineages evolved new TE lineages, we calculated the number of branch-specific TEs using RepeatMasker output. A TE was scored as "present" (score = 1) in a genome if at least 5,000 bp of sequence attributable to that TE was identifiable in the genomes of terminal branches. A TE was considered "absent" (score = 0) if fewer than 500 bp was identified. To score subclades, we allowed "possible presence" scores of 0.5 if base counts fell between the two values. Subclade "presence" sum threshold scores were subclade specific based on the number of species examined. For example, the erato subclade, with four members, had a presence sum of 3.5. Branch times were obtained using the median scores for each node calculated using TimeTree (Kumar et al. 2017). Rates of TE origination were calculated by dividing the number of branch-specific insertions by the time that the branch likely existed.

We estimated lineage-specific DNA contributions to selected branches of the tree by identifying DNA that was deposited by novel TEs that evolved on those branches. We then calculated both the genome proportions occupied by those elements and the total bp. For example, we summed the total contributions made by each of the 118 novel TEs identified in the *D. iulia* genome (table 2). Similarly, we summed total the total bp deposited by each novel TE identified on the eratosara common branch in each member of those clades and calculated the mean (supplementary file 1, Supplementary Material online).

Genome Size Correlations

Using the annotations generated, we compiled summary statistics of TE content in each heliconiine genome, in terms of TE bases per base pair (TE length) and number of insertions per base pair (TE count). We obtained genome size estimates from Edelman et al. (2018). Because the absolute values of these measures are several orders of magnitude apart, we Z-transformed each category by subtracting the mean and dividing by the SD.

PSMC Analyses

To examine historical effective population sizes in selected species, raw reads from the whole-genome sequencing data of selected species from each major clade were used. These include *H. melpomene*, *H. cydno*, *H. timareta*, *H. pardalinus*, *H. elevatus*, *H. hecale*, *H. numata*, and *H. besckei* when mapped to *H. melpomene* version 2.5; and *H. erato*, *H. himera*, *H. erato*×*H. himera* hybrid, *H. hecalesia*, and *H. demeter* when mapped to *H. erato demophoon* v1 (see supplementary fig. 13, Supplementary Material online). Reads were filtered for Illumina adapters using cutadapt v1.8.1 (Martin 2011) and then mapped to both *H. melpomene* version 2.5 and *H. erato demophoon* v1 using BWA mem v0.7.15 (Li 2013), with default parameters and marking short split hits as secondary. Mapped reads were sorted and duplicate reads removed using sambamba v0.6.8 (Tarasov et al. 2015). Mapped reads were further realigned around INDELs using the Genome Analysis Toolkit (GATK) v3.8 RealignerTargetCreator and IndelRealigner modules (McKenna et al. 2010; DePristo et al. 2011), to reduce the number of INDEL miscalls. Genotype calling was performed for each individual separately with bcftools v1.5 (Li et al. 2009) mpileup and call modules (Li and Durbin 2011), using the consensus-caller model (call -c) and requiring minimum base and mapping qualities of 20, and a minimum depth of 8. PSMC was run with parameters used in Martin et al. (2016), namely 25 iterations, with 29 interval parameters spread over 58 time intervals (command flag -p

"$28\times2+3+5$"). For plotting purposes, we used a generation time of 0.25 years and a mutation rate of 2×10^{-9}.

Results

Data

Draft genomes for 19 species were analyzed for TE content (fig. 1). Details of each assembly are available in Edelman et al. (2018) and in supplementary table 1, Supplementary Material online. One species, *H. melpomene*, has been analyzed thoroughly for TEs and therefore served as a starting point for some downstream analyses (Heliconius 2012; Lavoie et al. 2013). We assumed that any old, shared insertions among the species analyzed were identified as part of that analysis or are part of other insect TE libraries.

Novel and Known TE Families

After culling to eliminate duplicates and previously identified TEs, 93 novel DNA transposon consensus sequences, 59 novel LINE consensus sequences, 136 novel Helitron elements, and 65 novel LTR elements were identified. Among SINEs, the previously identified Metulj family was examined using a network-based approach (Levy et al. 2017). That analysis yielded 2,483 novel subfamilies, adding substantially to the Metulj diversity (~30 subfamilies) described in (Lavoie et al. 2013).

Three novel SINE families, which can be grouped as a new superfamily we are calling ZenoSINEs because of their presumed mobilization partner and other shared characteristics, were also identified. A fourth novel SINE family with similarities to R1 LINEs was also identified. All novel TE consensus sequences have been deposited in DFAM (Hubley et al. 2016).

Recent versus Ancient Taxonomic Distributions

Because our interest was in determining how TEs may be influencing genomic structure in modern species, we distinguished between recent and ancient accumulation patterns. RepeatMasker hits with divergences <0.05 from their respective consensus sequences were considered "recent" and >0.05 as "old." Applying a mutation rate of 1.9×10^{-9} substitutions/site/generation and 4 generations/year (Martin et al. 2016) and assuming minimal differences among species places this boundary at ~6.6 Ma, allowing us to focus on accumulation patterns in the melpomene-sylvaniformes and erato-sara clades as well as the terminal branches leading to *Heliconius doris*, *Heliconius burneyi*, and the three outgroup taxa (fig. 1). For each TE (separated by names, class, or family, depending on the level of analysis), total base coverage was calculated and divided by the total genome size to give a relative proportion (fig. 2). The figure illustrates the distinct shift from SINE dominance in ancestral accumulation patterns toward RC, LINE, and DNA dominance in the melpomene and sylvaniform clades in addition to distinct patterns in several additional species. Unpaired *t*-tests comparing all members of the erato-sara clade to melpomene-sylvaniform species indicates significant differences between accumulation patterns of recent SINE, LINE, DNA transposon, and RC transposons insertions by class, $P<0.0001$, $P=0.0229$, $P=0.0078$, $P=0.0008$, respectively.

Examining TE accumulation at a finer scale reveals additional patterns. For example, while recently accumulating RC transposons (Helitrons) contribute to all genomes, those contributions vary substantially (fig. 3), ranging from almost no Helitron content in *Agraulis vanillae* and *H. doris* to near complete dominance in all members of the melpomene and sylvaniform clades. Further, there are clear differences in which subfamilies of Helitron have mobilized (supplementary figs. 1 and 2, Supplementary Material online). Not surprisingly, the Helitron-like elements first described by Lavoie et al. and discovered in the *H. melpomene* genome are prevalent in the melpomene and sylvaniform clades, particularly *Heliconius elevatus* and *Heliconius pardalinus*. Distinct Helitron subfamilies have recently colonized species in the erato, sara, and doris clades but with less success.

Similarly, many DNA transposons have had substantially more recent success in mobilizing within the doris, melpomene, and sylvaniform clades, again with distinct families being more prevalent, depending on the lineage (fig. 3). The most obvious difference with regard to DNA transposons lies in the increased prevalence of PIF-Harbinger, piggyBac, hAT, and most TcMariner superfamily transposons in certain clades (fig. 3 and supplementary figs. 1 and 3, Supplementary Material online), especially melpomene and sylvaniform. TcMariner elements also appear to be the only DNA transposons to have managed any success in the *H. burneyi* and *H. doris* genomes while *Eueides tales* and *Heliconius sara* seem to have avoided any substantial DNA transposon accumulation in the recent past.

Recent LTR retrotransposon accumulation patterns exhibit similar diversity (fig. 3 and supplementary figs. 1 and 4, Supplementary Material online). Despite the fact that there is not a significant difference in overall accumulations between members of the combined erato-sara clade and species in the combined melpomene-sylvaniform clade (unpaired *t*-test, $P=0.2804$), there is a distinct bias toward Gypsy retrotransposons and a subset of generic LTRs in the melpomene and sylvaniform clades while a subset of LTR retrotransposons are preferred in species of the erato and sara clades as well as in *A. vanillae*. As with Helitrons and DNA transposons, the identities of the LTR retrotransposons that have expanded in each group are distinct (supplementary fig. 4, Supplementary Material online).

Recent accumulation by LINEs is diverse but most prominent in *H. doris*, with CR1, Zenon, and RTE elements dominating other LINEs (fig. 3 and supplementary fig. 5, Supplementary Material online). Clades to the left in figure 3

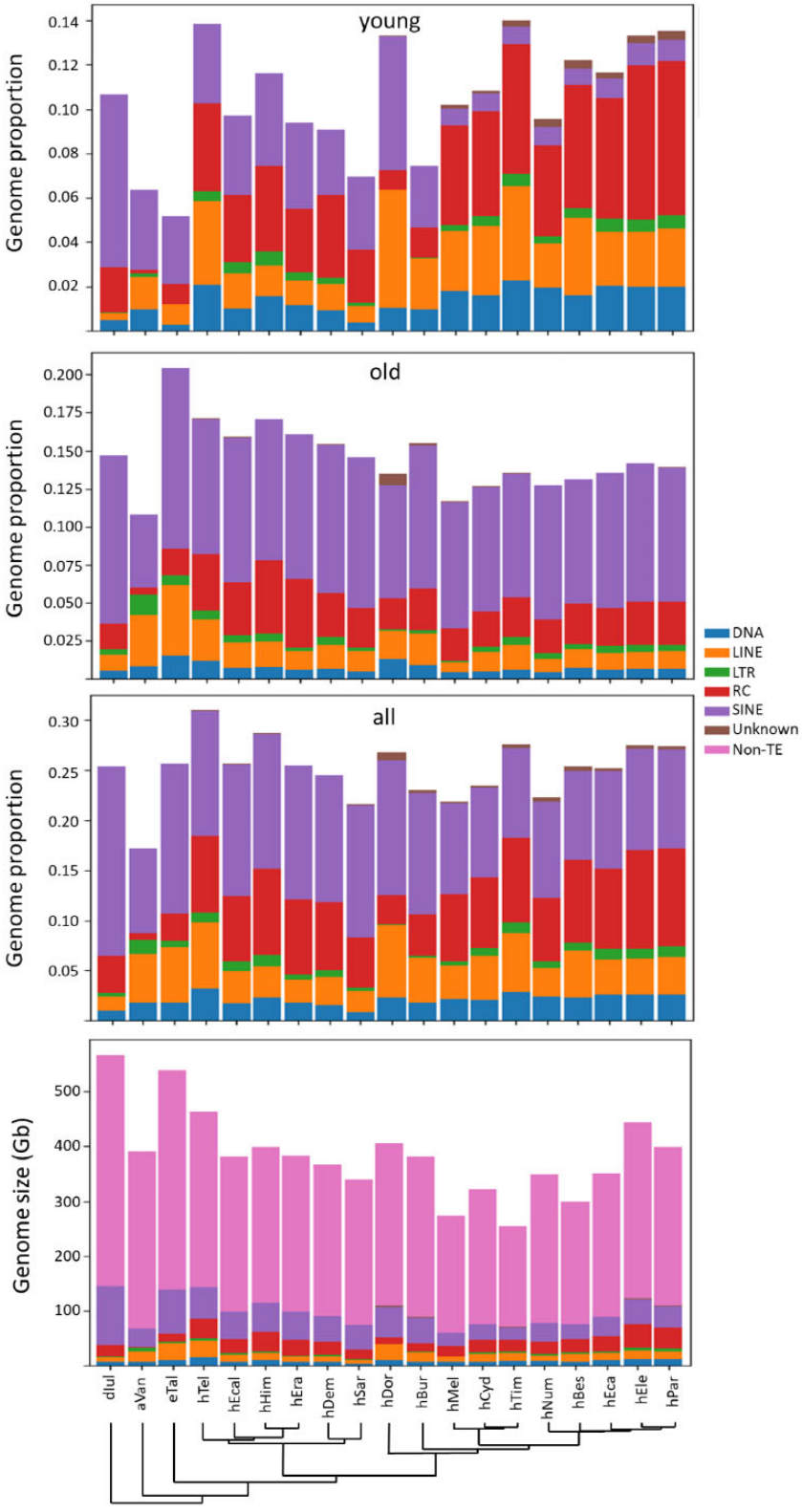

Fig. 2.—Stacked bar plots of TE proportions categorized as "old," "young," and "all" in each species examined. The combined plot at the bottom represents all data in the context of genome size. Species and their phylogenetic relationships (fig. 1) are depicted on the *x* axis. Abbreviations are as described in supplementary table 1, Supplementary Material online. Briefly, the first letter indicates genus, and the following three (or four) letters, except in the cases of *Heliconius hecale* and *H. hecalesia*, indicate species as listed in figure 1. Values on the *y* axis are genome proportions calculated as described in the text or total bp representation.

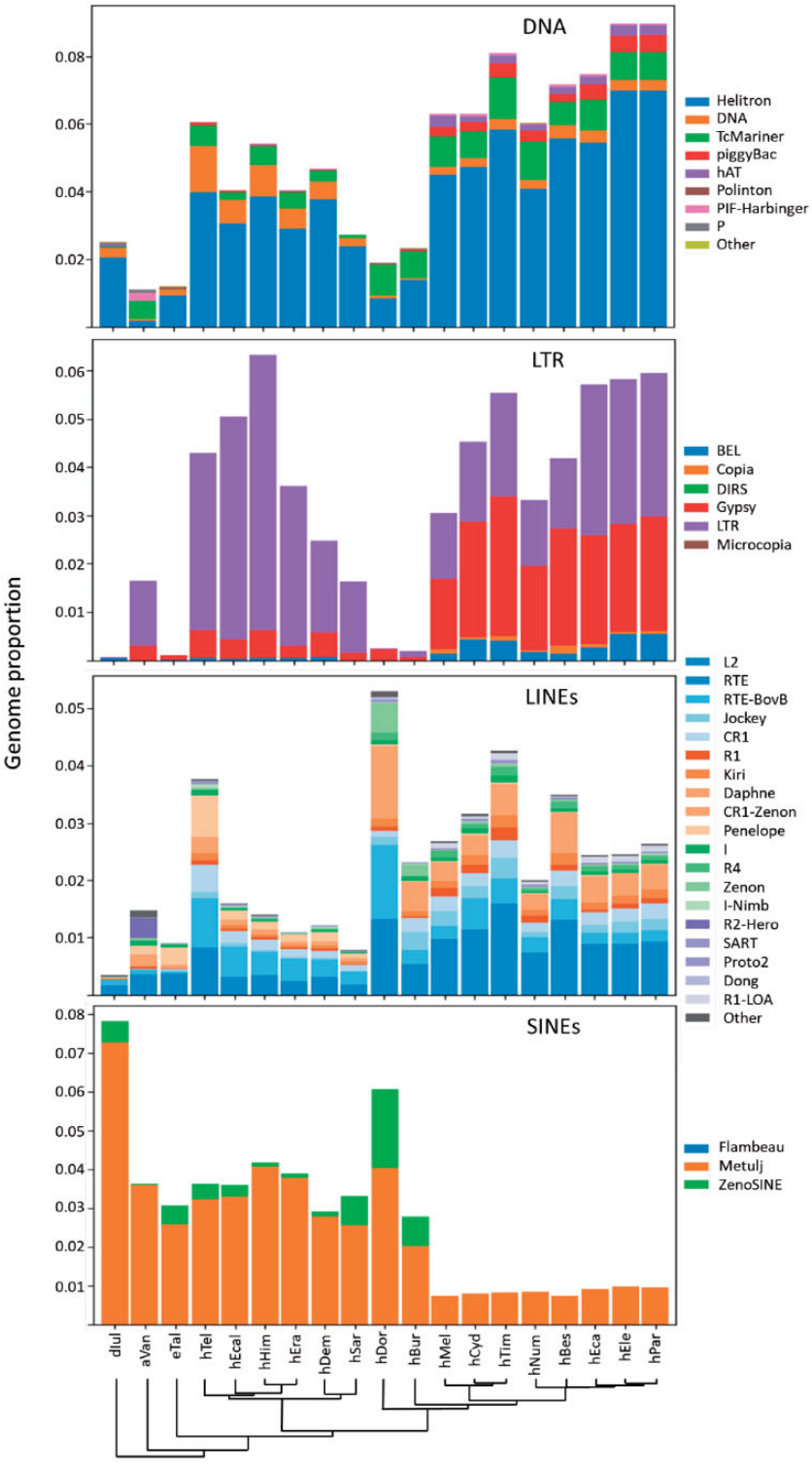

Fig. 3.—Recent contributions to genome content from each of the four TE classes examined. Axes and abbreviations are as described in figure 2. Rolling circle (RC) transposons, Helitrons, are depicted as part of the DNA transposon plot.

have generally experienced much lower levels of recent non-LTR retrotransposon accumulation. In these clades, though, a variety of short, nonautonomous Penelope elements are much more prominent, especially in *Heliconius telesiphe*. R2-Hero elements make up a large relative proportion of LINE-occupied space in *A. vanillae*. As with the previous

classes, LINE identities are highly lineage-specific (supplementary figs. 1 and 5, Supplementary Material online).

In many genomes, SINEs are the most prevalent TE component by genome proportion. As is apparent in figure 2 and supplementary figure 6, Supplementary Material online, this is also the case for several heliconiines. The Metulj family make the most significant recent contributions in clades other than melpomene and sylvaniform. ZenoSINEs are present only in those same clades. *Heliconius doris* is an exception, with nearly as much accumulation from ZenoSINEs as from Metulj. Indeed, the distribution of ZenoSINEs is a puzzle. In addition to their presence in *H. doris*, and to a lesser extent *H. burneyi*, they are found primarily in *E. tales* and members of the *erato* and sara clades. ZenoSINEs are essentially absent from members of the melpomene and sylvaniform clades (table 1). We examined the raw RepeatMasker output from each genome for the presence of any ZenoSINE elements >100 bp in length. Counts ranged from 5 to 21 in the melpomene and sylvaniform clades. Sixty-two were found in *A. vanillae*, and only 12 were identifiable in *Dryas iulia*. Examination of the extracted hits on a clade by clade basis reveals that relatively few are likely to be genuine ZenoSINE elements. All of the hits from *A. vanillae* and members of the melpomene and sylvaniform clades were about half the size of the average ZenoSINE consensus, truncated at the 5′ end. For hits in the *D. iulia* genome, the hits were also short but the truncation occurred at the 3′ end. We suggest that the vast majority, if not all, such low-copy number hits in table 2 follow are similarly false positives.

Table 1

Total Numbers of SINE Insertions >100 bp Present from Each Family Described in the 19 Genomes Examined

	Counts					
Taxon	Brushfoot	Flambeau	Fritillar	Julian	Metulj	ZenoSINE
dIul	385	134	10	16505	555536	16907
aVan	13	3	1248	4	172584	80
eTal	21	0	7	12	429689	11618
hTel	7	8	0	2	301411	6405
hEcal	2	4	1	0	261271	4172
hHim	6	8	0	0	280969	1492
hEra	0	0	0	0	266446	1440
hDem	4	0	0	0	248026	2012
hSar	0	1	0	0	231573	9139
hDor	14	0	0	0	250770	30999
hBur	15	0	0	1	243679	11912
hMel	2	0	0	0	147575	7
hCyd	5	0	0	0	172064	18
hTim	3	0	0	0	135749	15
hNum	4	0	0	0	200506	14
hBes	5	0	0	0	160502	25
hEca	6	1	0	0	204966	28
hEle	10	1	0	0	266629	32
hPar	6	0	0	0	232673	21

NOTE.—Color coding indicates relative counts, darker green depicts higher numbers in each category.

Besides ZenoSINEs, four additional new families were identified. Two of these, Flambeau, and Julian SINEs are restricted to *D. iulia*. Brushfoot is also restricted to *D. iulia* within heliconiines but has some resemblance to a possible cousin in the genome of the pierid butterfly, *Leptidea sinapis*. Fritillar SINEs are restricted to the *A. vanillae* genome. With the exception of Julian, all are present at relatively low numbers (table 1). Further, our analysis of the rates of evolution of new TE lineages suggests that the erato-sara common ancestor, *H. doris*, and the outgroups were hotbeds of new SINE subfamily emergence (table 2), each associated with dozens of new subfamilies, while the melpomene and sara clades are host to a single novel subfamily.

SINE/LINE Partnerships

The 3′ ends of SINEs are often very similar to their LINE partner (Ohshima and Okada 2005). Previous efforts by Lavoie et al. (2013) were unsuccessful in determining the LINE partner for Metulj, but based on our more complete analysis of the TE content of all 19 genomes, we now suspect that it is mobilized by an RTE family LINE (supplementary fig. 7*A*, Supplementary Material online). ZenoSINE, Fritillar, and Flambeau show similarity between their tails and the tail of LINEs from the Zenon family (supplementary fig. 7*B*, Supplementary Material online), suggesting a similar relationship. Flambeau exhibits 3′ similarity with R1 LINEs (data not shown).

Table 2

TE Origination Rate Calculations for Relevant Terminal and Internal Branches on the Heliconiine Tree (fig. 1)

Branch	Branch Time	Threshold score	Branch-specific TEs	TE origination Rate	DNA	RC	LTR	LINE	SINE	Space contribution (Mb)
D. iulia	26.2 mya - present	1	136	5.19	6	7	0	7	118	85.2
A. vanillae	23.8 mya - present	1	58	2.44	7	2	1	22	29	35.7
E. tales	18.4 mya - present	1	58	3.15	3	3	0	15	41	36.9
Heliconius ancestral branch	18.4 mya- 11.1 mya	14	2	0.27	0	1	0	1	0	not examined
erato-sara ancestral branch	11.1 mya - 5.8 mya	5.5	102	19.32	2	7	2	3	88	23.9
erato ancestral branch	5.8 mya - 4.7 mya	3.5	9	1.55	2	2	2	0	3	not examined
H. telesiphe	4.7 mya - present	1	3	0.64	1	0	0	0	2	not examined
H. demeter	5.0 mya - present	1	1	0.20	0	0	0	0	1	not examined
H. sara	5.0 mya - present	1	4	0.80	0	1	0	0	3	not examined
H. doris	11.1 mya - present	1	104	9.37	0	2	0	15	91	22.3
H. burneyi	6.6 mya - present	1	15	2.26	3	0	0	6	8	not examined
melpomene-sylvaniform ancestral branch	6.6 mya - 2.8 mya	7.5	130	34.67	31	20	13	65	1	23.4

NOTE.—Color coding indicates relative counts and rates, darker green depicts higher numbers in each category.

The SINE tail may influence the success of the SINE in hijacking the LINE enzymatic machinery at the ribosome (Dewannieux and Heidmann 2005). Our investigations into the evolution of the 3′ tail revealed informative patterns (supplementary fig. 8, Supplementary Material online). In most *Heliconius*, young Metulj show a distinct bias toward A and T over G and C and A:T ratios are biased slightly toward T in young insertions, a signal not observed in older elements. The A prevelance over C and G is slightly higher in members of the erato and sara clades and distinctly higher in *D. iulia*, *A. vanillae*, and *H. doris*.

Because of the apparent partnership that has evolved between these SINEs and their partner LINEs, one might expect similar recent accumulation profiles. However, no relationship between the accumulation patterns is easily resolvable (fig. 4). Indeed, while there does appear to be some mirroring in *H. doris*, *H. burneyi*, and possibly in the erato and sara clades, the accumulation patterns observed in melpomene and sylvaniform are essentially opposite. A similar lack of correspondence in landscapes is apparent for ZenoSINE and Zenon LINEs. Examining correllations between recently accumulated SINEs and LINEs also reveals no discernable pattern (supplementary fig. 9, Supplementary Material online). While the expected high correspondence between ZenoSINE and Zenon LINEs is observed, so are high correlations with Dong and RTE-BovB. Further, the expected correlation between RTE-type LINEs and Metulj is not observed.

SINE Birth and Death

Four of the novel SINEs likely originated recently within the Heliconiini. A BLAST search of all taxa excluding *Heliconius* in the NCBI WGS database using ZenoSINE consensus sequences yields only severely truncated and low similarity hits in the genomes of other lineages. Analysis of Fritillar suggested that it is restricted to *A. vanillae*, strongly suggesting that it originated in that lineage. The BLAST search produced 12 high similarity, partial hits to the fellow nymphalid butterfly *Vanessa tameamea* (the Kamehameha butterfly, GCA_002938995.1). The hits are limited to the 5′ (likely tRNA-derived) half of the SINE suggesting that these are merely hits to a similar precursor tRNA in that genome.

ZenoSINE subfamilies are similarly restricted to a subset of heliconiine lineages (figs. 3 and 4), suggesting an origin near the base of the heliconiine clade. Our BLAST search yielded hits only to *Heliconius aoede* (GCA_900068225.1), which is sister to the doris–wallacei–melpomene–sylvaniform assemblage. Questions that will be addressed below exist on how the current distribution came to be.

Metulj are present in all species examined, suggesting that their origin is more ancient but at least prior to the diversification of the Heliconiini. A BLAST search of the NCBI WGS database yields hits only in heliconiine genomes thus far deposited with NCBI. Similar results are obtained by a broader search of all insect nucleotides in the database. Thus, while a specific point of origin cannot be identified, we suggest that Metulj originated with the clade or shortly thereafter. The lack of any substantial recent accumulation in members of the melpomene and sylvaniform clades (fig. 3) strongly suggest that Metulj is dead or dying in those lineages.

TE Origination Rates

Table 2 details the rates at which various branches in the phylogeny gained novel TEs. In agreement with much of the data presented earlier, the erato and sara clades along with *H. doris* and the three outgroups have been home to intensive SINE diversification while the melpomene and sylvaniform clades have played host to origination events for most other categories. The highest rates of TE origination appear to center on the ancestors of each of the two major subclades and in *H. doris*.

Using this information, we determined amounts of lineage-specific TE-derived DNA contributions along selected branches of the tree (supplementary file 1, Supplementary Material online). Substantial contributions to genome diversity were observed. For example, at least 15% (~85 Mb) of the *D. iulia* genome is uniquely TE-derived when compared with any other species analyzed with most of that content (~11%, ~62 Mb) derived from lineage-specific SINEs. Around 5.5% (22 Mb) of the *H. doris* genome is unique to that lineage. Clade-specific TE contributions to the erato-sara and melpomene-sylvaniform clades are similar, averaging 5.9% (~24 Mb) and 6.9% (~23 Mb), respectively. Not surprisingly given the observations above, those contributions are quite distinct, with SINEs making up the majority of novel DNA (~15 Mb) in the erato-sara clade and DNA transposons comprising the majority (~18 Mb) in members of melpomene and sylvaniform.

PSMC Analyses of Historical Effective Population Size

The CArrier SUbpopulation (CASP) hypothesis of Jurka et al. (2011) suggests that current TE diversity in a genome could be driven primarily by historical population subdivision, that is, increased historical population subdivision is positively correlated with increased current TE diversity. To test this prediction, we estimated historical (N_e) using the Pairwise Sequentially Markovian Coalescent (PSMC) model. For all species we tested, a reduction in effective population sizes, which could be indicative of increased population subdivision, is apparent between ~40,000 and 100,000 years ago.

Genome Size Correlations

Recently, Talla et al. (2017) found that genome size in woodwhite butterflies (Leptidea) correlated strongly with TE accumulation. To determine if the same phenomenon was observable in heliconiines, we followed Talla et al. (2017) and

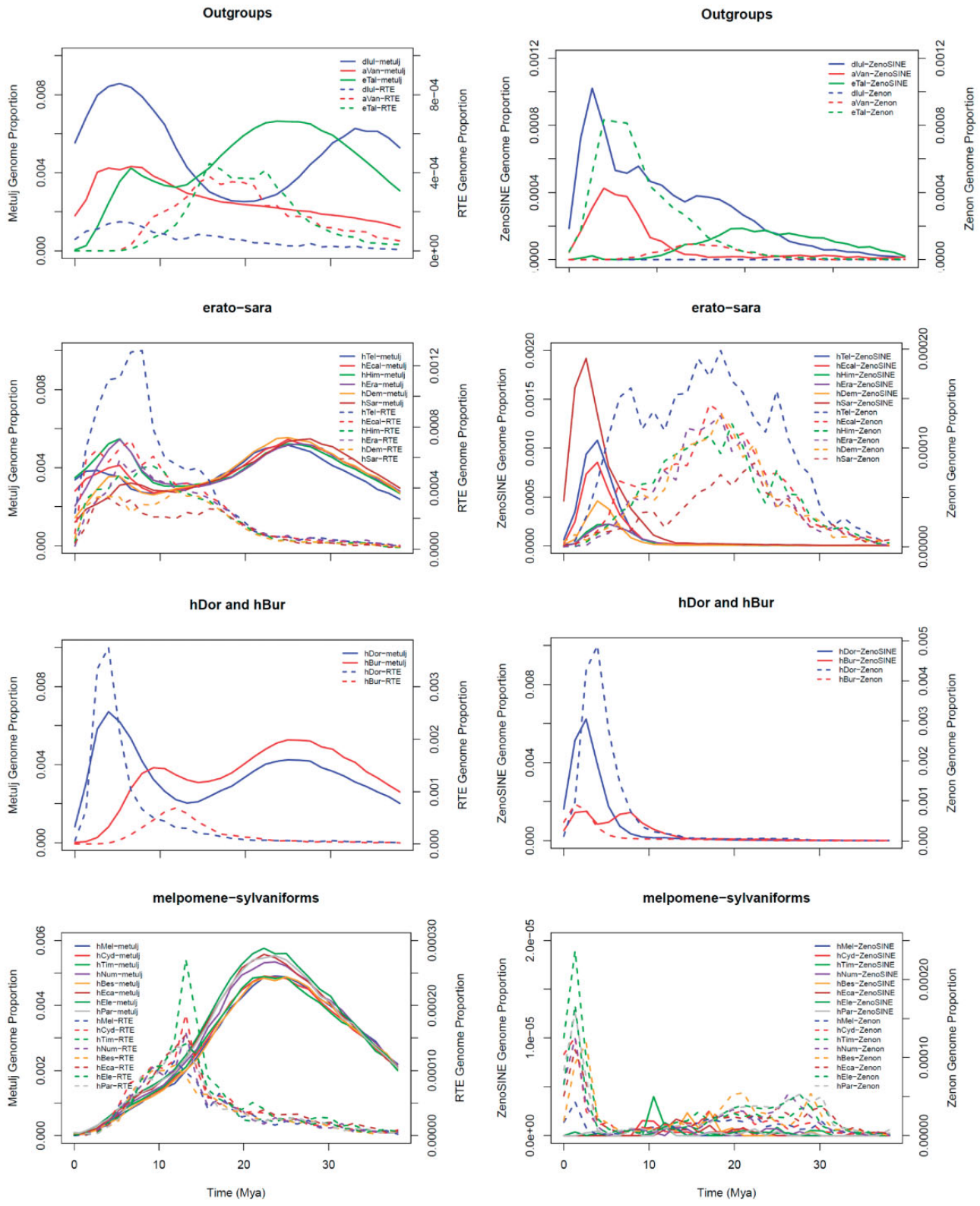

Fig. 4.—TE landscape plots for Metulj-RTE partners (left column) and ZenoSINE-Zenon partners (right column) in the four species divisions analyzed. The *x* axis depicts the estimated time of accumulation of the TE using the mutation rate described in the text. *y* axes depict genome proportions occupied by the TE for any given time on the *x* axis. Values for SINE-derived DNA are on the left axes and values for LINE-derived DNA are on the right axes.

calculated a linear model of genome size as a function of TE length, and found no significant correlation ($P = 0.11$). However, we did find a marginally significant correlation of genome size with TE count ($P = 0.0165$). We repeated the analysis accounting for phylogenetic relatedness using the *pic* function in the R package ape v5.1 using a tree generated from concatenated, noncoding, fully aligned regions to perform the phylogenetic correction (Edelman et al). Our results were consistent, though for both comparisons relatedness did account for some of the variation (TE length $P = 0.306$, TE count $P = 0.0275$). All following analyses were performed with this phylogenetic correction.

Because these species diverged very recently, we hypothesized that recent insertions may be more relevant for differences in genome size. However, this was not consistent with the data. When only considering TE insertions with divergence values <0.05, we found no association of genome size with either TE length ($P = 0.0891$) or TE count ($P = 0.482$).

To determine if any one element could be influencing genome size evolution, we next classified each insertion based on both class and family and analyzed each independently. For the full data (recent and old elements), after correcting for multiple comparisons, only I.Nimb elements were significantly associated with genome size (I.Nimb length $P = 5.17e^{-5}$, I.Nimb count $P = 8.76e^{-5}$). However, I.Nimb elements make up only a small fraction of the genome, and the pattern appears to be driven by two outliers, *H. telesiphe* and *E. tales* (supplementary fig. 10, Supplementary Material online). For the recent elements, again a single element, Penelope, is associated with genome size (supplementary fig. 11, Supplementary Material online), but here the association is with count alone, and again it appears to be driven by the high density of Penelope in *H. telesiphe* (Penelope length $P = 0.059$, Penelope count $P = 1.1e^{-4}$).

Discussion

TE distributions and expansion dynamics can reveal vital information about evolutionary processes. For example, taxonomic disparities in the distribution of a TE family is a sign of possible horizontal transfer among disparate lineages. The presence of high numbers of orphaned TE fragments is an indicator of high rates of nonhomologous recombination that acts to remove DNA from the genome, impacting genome sizes. Thus, detailed examinations of TE content are an important step in understanding how genomes evolve. This work is the first large-scale, comprehensive analysis of TE dynamics in a coherent clade and reveals substantial information on how TEs play into heliconiine genome diversification. Our analysis of recent accumulation patterns reveals that clear taxonomic differences have evolved with regard to the relative success of TE families across the clade.

The most obvious differences are apparent shifts in TE success in proliferating in each clade. A basal divergence in TE accumulation has evolved in *Heliconius*, with members of the melpomene and silvaniform clades showing a bias for RC transposons, DNA transposons, and LINEs. Meanwhile, their cousins in the erato and sara clades have been host to substantial recent SINE accumulations. Two other *Heliconius* species examined appear to have undertaken divergent strategies. *Heliconius doris* seems to split the difference between the "right" and "left" clades in figure 3 in allowing substantial accumulation from both SINEs and LINEs in the recent past while *H. burneyi* has restricted the proliferation of nearly all TEs without regard to class membership.

SINEs are often the most numerous TEs in eukaryotes. For example, while LINEs outstrip SINEs in the human genome by mass, the number of SINE insertions in our genomes surpasses LINEs by an order of magnitude (Lander et al. 2001). With such high copy numbers, SINEs are responsible for significant structural changes and therefore deserve special attention (Wang and Kirkness 2005). SINEs are also relatively short-lived residents of many genomes, often showing higher lineage-specificity when compared with their LINE partners. This pattern is observed in the present study as we can identify all three phases of a SINE life cycle, birth, expansion, and (potentially) death.

Examination of Metulj elements suggest an interesting history. Their unambiguous presence in all species makes it clear that they evolved in the common ancestor of Heliconiini. However, their recent expansion is restricted to only a subset of the taxa examined. This suggests lineage-specific mechanisms acting to either silence this family either through active mechanisms or via self-downregulation or through massive increases in SINE mobilization. Depicting the data as TE landscapes suggests a combination of these mechanisms (fig. 4). Applying the neutral substitution rate of Martin et al. (2016) to divergence values, one can see that all members of *Heliconius* and *E. tales* experienced a peak of Metulj activity ~25 Ma. This timing corresponds well with the time that a common ancestor of these species existed (fig. 1). After the initial *Heliconius* divergence, all species exhibit a decline in TE accumulation as one moves toward the present, but this is followed by resurgences in all lineages except of melpomene and silvaniforms. Indeed, the lack of variability in recent Metulj content (fig. 3) suggests a rapid cessation of activity in the common ancestor of these clades.

The reason for the death of Metulj in the latter clades is unclear, as is the cause of the resurgence in other species. Why any SINE goes extinct is unknown and could be influenced by multiple factors including genomic defenses, the quiescence of the partner LINE, mutations in the SINEs themselves, and population genetic processes (see below). The evolution of new subfamilies requires mobilization of the elements. Thus, the lack of any new subfamilies that are unique to this clade suggests a cessation of retrotransposition. If we are correct in our conclusion that RTE LINEs are responsible for Metulj mobilization, some clues may be found by

examining those elements. One potential explanation is to view the SINE-LINE relationship not as a partnership but as a competition for the enzymatic machinery produced by LINEs. If the SINEs are particularly effective at hijacking that machinery, it may be possible for them to suppress LINE mobilization to some extent, even to the eventual demise of the LINE partner, as was recently hypothesized in sigmodontine rodents (Yang et al. 2019). Our analysis of Metulj tails suggests that the ancestral tail of Metulj SINEs was A-rich and that a switch toward tails containing more T residues may be involved in the success of this SINE in the erato and sara clades. This hypothesis does not, however, hold true for *D. iulia*, *A. vanillae*, or *H. doris*, which have all experienced high rates of recent Metulj accumulation but exhibit a bias toward A nucleotides in their tails. These results suggest that the reasons for the differential success in heliconiine genomes may be many, and complex.

Not surprisingly, the outgroup species, with their deeper divergences, exhibit their own unique patterns. *Dryas iulia*, with the highest proportion of Metulj in its genome, experienced a recent surge in accumulation that outpaced any other heliconiine examined. *Eueides tales* mirrors the erato and sara clades while *A. vanillae* appears to have experienced a gradual increase in accumulation very recently.

Previous analyses (Lavoie et al. 2013) suggested that larger TEs in *Heliconius* genomes are removed via nonhomologous recombination. This hypothesis is not refuted by our data. Examination of the TE landscape plots described earlier suggests that, unlike the pattern observed in mammalian genomes, where TEs remain as molecular fossils over large swaths of evolutionary time (Lander et al. 2001; Waterston et al. 2002), there is substantial turnover of TEs in these butterfly genomes. For example, when examining the temporal accumulation landscapes of Metulj, a SINE that averages well under 300 bp, we can readily see evidence of ancient accumulation (fig. 4). The LINE TE classes exhibit much less clear signatures: we rarely see ancient peaks in accumulation plots (supplementary fig. 12, Supplementary Material online). This suggests that these genomes can rapidly diverge over evolutionary time once reproductive isolation is acquired, with distinct lineages retaining little ancient TE-derived homology from larger elements across their genomes.

Assuming the phylogeny proposed by Kozak et al. (2015) and Edelman (submitted), the distribution of ZenoSINE elements is difficult to explain. The family is present at substantial numbers in *E. tales*, all members of the erato and sara clades, *H. doris*, and *H. burneyi*. Such a distribution could be explained by at least two scenarios. First is an ancient origin for the family in the common ancestor of the monophyletic group that includes *E. tales* and all members of *Heliconius* followed by not just a loss of activity in the melpomene and silvaniform clades but also by the removal of any previously existing insertions. The lack of any genuine ZenoSINEs (see Results) in these genomes makes this "ancient origin" hypothesis less likely. Second, it is possible that ZenoSINE evolved in only one of these lineages and this was followed by migration, either through horizontal transfer or hybridization, to the others. For example, one such scenario would be that this SINE evolved in the common ancestor of the erato and sara clades and managed to move to the other species in which it is found. Given the high tendency toward hybridization in the *Heliconius* overall (Mavarez et al. 2006; Kronforst 2008; Heliconius 2012; Nadeau et al. 2012), this seems the more plausible scenario. However horizontal transfer, given that it could be a common phenomenon in insects (Peccoud et al. 2017), cannot be ruled out.

Rates of TE origination in Heliconiini follow some expected patterns. *Dryas iulia*, with the longest branch on the tree has the highest fraction of branch-specific TEs (table 2). This would be expected given a relatively constant rate of TE origination and the ancient divergence that it represents. However, examination of *Heliconius* suggests that TE origination rates are not uniform along the tree. Instead, there is a burst of TE evolution during the early stages of *Heliconius* diversification, in particular on the branch leading to the melpomene and silvaniform subclades, which spans a period ranging from ~7–3 Ma. This corresponds well with the findings of Kozak et al. who identified a rapid increase in species diversification during the same period (Kozak et al. 2015). Those authors proposed that environmental perturbation allowed for the invasion of new niches. This also corresponds with the periods of extensive cross-lineage hybridization found by Edelman et al. Collectively, this suggests that TEs may have been shuffled between lineages during this time. Such mixing could lead to "mismatching" in TE content versus TE defense machinery and subsequently permitted the extensive accumulation of different TEs in different lineages. While we do not yet have data to support such a scenario, similar mismatches have been shown to play a role in *Drosophila* reproductive isolation (Petrov et al. 1995).

Indeed, these observations suggest potential differences in the ways that each species deals with genomic stress caused by TE mobilization and that TE defense strategies diverge rapidly in each lineage. This is consistent with the model of piRNA clusters acting as TE "traps" in which, upon an element's insertion into a cluster, a piRNA-based defense against that element is mounted (Lu and Clark 2010). As *Heliconius* butterflies diversified, different TEs would be expected to have fallen into piRNA traps evolving in each lineage, leading to different levels of response. This would yield clade-specific patterns similar to those observed here. With the detailed descriptions we have provided, this is a hypothesis that could eventually be tested.

TEs have been shown to respond to environmental stressors, thereby leading to substantial genomic instability (Rey et al. 2016). Such instability has the potential, in turn, to provide novel genotypes and phenotypes upon which selection can act, either through direct changes to coding regions (Clark et al. 2006) or through perturbations of gene

regulatory pathways (Chuong et al. 2016, 2017; Trizzino et al. 2017). We suggest that the geologic and climatic upheaval described for this period (Gregory-Wodzicki 2000; Hoorn et al. 2010; Jaramillo et al. 2010; Rull 2011; Blandin and Purser 2013), may have set this cascade into motion in Heliconiini. Indeed, one recent study found that regulatory elements that differed between the sister species *Heliconius erato* and *Heliconius himera* were enriched for LINE content (Lewis and Reed 2018), suggesting an impact by LINEs on regulatory innovation.

Conversely to the above hypotheses, Jurka et al. (2011) suggest that TEs should more accurately be viewed as "drifters accompanying population subdivision rather than the drivers of speciation." We cannot rule this out. Nor can we provide evidence in support of this scenario. The recent apparent reductions in overall N_e could help explain the high TE diversity in the erato, sara, melpomene, and silvaniform clades but confident inferences are difficult. Short generation times in butterflies obscure N_e estimates past ~1 Ma (supplementary fig. 13, Supplementary Material online). That said, we cannot rule out a role for TE-driven diversification, even if the TEs themselves are not playing an active role in generating selectable traits.

Indeed, the observations presented here make it clear that differential TE activity and accumulation can act as a force for rapid genomic divergence regardless of whether they are drivers or passengers. Similar analyses of multiple taxa have been performed for other groups including squamates and birds (Kapusta and Suh 2017; Pasquesi et al. 2018). In those studies, especially the squamates, similar shifts in TE content and accumulation were observed. However, those analyses examined much deeper divergences than the ones examined here. In examining much more closely related lineages, we demonstrate that the TE landscapes in members of a single genus can diverge rapidly due to differential TE dynamics. Lineages whose common ancestor harbored a single complement of TEs now play host to very distinctive complements of recently active TEs with patterns that resemble genomic fingerprints. Even in the case of LTR accumulation, where no significant difference exists with regard to overall accumulation amounts, the identities of the elements that have accumulated are quite distinct. Such distinctions are true of all classes. This is exemplified by our observation that on an average ~23 Mb (5.3–9.2%, depending on genome size) of the genomes of the melpomene and silvaniform subclades harbor TE-derived DNA that would not be found in members of erato and sara. In *D. iulia*, a full 15% (85.2 Mb) of the genome is uniquely TE-derived in that lineage when compared with any other species we examined. The data make it clear that novel TE families, such as ZenoSINE and Julian, can arise and replicate rapidly to occupy substantial genome fractions in isolated lineages. Furthermore, because these genomes tend to actively remove longer TEs, the ancestral fractions of each genome will change rapidly as different portions are removed in each lineage.

Here, we provide what amounts to a 'natural history' of TEs in the genomes of 19 relatively closely related species. Researchers interested in how TE related factors impact the evolution of genome structure and function now have a detailed starting point from which to begin detailed studies. These results suggest powerful ways to move forward in understanding the forces that TEs exert on genome evolution and the forces that act in turn to regulate TE activity. For example, the purely structural component of genome evolution, when combined with potential functional impacts of TEs as they contribute new open reading frames, regulatory sites, and small RNAs add support to the contention that TEs are major drivers of genome evolution and deserve significant attention when determining the forces that lead to the taxonomic and phenotypic diversity around us.

Supplementary Material

Supplementary data are available at *Genome Biology and Evolution* online.

Acknowledgments

The authors wish to thank the College of Arts and Sciences at Texas Tech University for funding related to this work. In addition, we would like to thank the Texas Tech HPCC (http://www.depts.ttu.edu/hpcc/) for providing computational resources necessary to complete this project. Angela Peace provided assistance with early conceptual analyses. The 20-genome *Heliconius* project was funded by a SPARC Grant from the Broad Institute of Harvard and MIT as well as startup and studentship funds from Harvard University. Fernando Seixas provided valuable assistance with the PSMC analysis. Support for DAR was provided by the National Science Foundation (DEB1838283).

Literature Cited

Altschul SF, Gish W, Miller W, Myers EW, Lipman DJ. 1990. Basic local alignment search tool. J Mol Biol. 215(3):403–410.

Arias CF, et al. 2017. A new subspecies in a *Heliconius* butterfly adaptive radiation (Lepidoptera: Nymphalidae). Zool J Linn Soc. 180(4):805–818.

Blandin P, Purser B. 2013. Evolution and diversification of Neotropical butterflies: insights from the biogeography and phylogeny of the genus Morpho Fabricius, 1807 (Nymphalidae: Morphinae), with a review of the geodynamics of South America. Trop Lepid Res. 23:62–85.

Capella-Gutierrez S, Silla-Martinez JM, Gabaldon T. 2009. trimAl: a tool for automated alignment trimming in large-scale phylogenetic analyses. Bioinformatics 25(15):1972–1973.

Carbone L, et al. 2014. Gibbon genome and the fast karyotype evolution of small apes. Nature 513(7517):195.

Chuong EB, Elde NC, Feschotte C. 2016. Regulatory evolution of innate immunity through co-option of endogenous retroviruses. Science 351(6277):1083–1087.

Chuong EB, Elde NC, Feschotte C. 2017. Regulatory activities of transposable elements: from conflicts to benefits. Nat Rev Genet. 18(2):71–86.

Clark LA, Wahl JM, Rees CA, Murphy KE. 2006. Retrotransposon insertion in SILV is responsible for merle patterning of the domestic dog. Proc Natl Acad Sci U S A. 103(5):1376–1381.
DePristo MA, et al. 2011. A framework for variation discovery and genotyping using next-generation DNA sequencing data. Nat Genet. 43(5):491.
Dewannieux M, Esnault C, Heidmann T. 2003. LINE-mediated retrotransposition of marked Alu sequences. Nat Genet. 35(1):41–48.
Dewannieux M, Heidmann T. 2005. Role of poly(A) tail length in Alu retrotransposition. Genomics 86(3):378–381.
Edelman NB, Frandsen PB, Miyagi M, et al. 2018. Genome architecture and introgression shape a butterfly radiation. bioRxiv 466292; doi: https://doi.org/10.1101/466292.
Edgar RC. 2004. MUSCLE: multiple sequence alignment with high accuracy and high throughput. Nucleic Acids Res. 32(5):1792–1797.
Ellison CE, Bachtrog D. 2013. Dosage compensation via transposable element mediated rewiring of a regulatory network. Science 342(6160):846–850.
Grabundzija I, et al. 2016. A Helitron transposon reconstructed from bats reveals a novel mechanism of genome shuffling in eukaryotes. Nat Commun. 7(1).
Gray YH. 2000. It takes two transposons to tango: transposable-element-mediated chromosomal rearrangements. Trends Genet. 16(10):461–468.
Gregory-Wodzicki KM. 2000. Uplift history of the Central and Northern Andes: a review. Geol Soc Am Bull. 112(7):1091–1105.
Hall TA. 1999. BioEdit: a user-friendly biological sequence alignment editor and analysis program for Windows 95/98/NT. Nucleic Acids Symp Ser. 41:95–98.
Hedges DJ, Deininger PL. 2007. Inviting instability: transposable elements, double-strand breaks, and the maintenance of genome integrity. Mutat Res. 616(1–2):46–59.
Heliconius GC. 2012. Butterfly genome reveals promiscuous exchange of mimicry adaptations among species. Nature 487:94–98.
Hoorn C, et al. 2010. Amazonia through time: Andean uplift, climate change, landscape evolution, and biodiversity. Science 330(6006):927–931.
Hubley R, et al. 2016. The Dfam database of repetitive DNA families. Nucleic Acids Res. 44(D1):D81–D89.
Jacques PE, Jeyakani J, Bourque G. 2013. The majority of primate-specific regulatory sequences are derived from transposable elements. PLoS Genet. 9(5):e1003504.
Jaramillo C, et al. 2010. Amazonia, landscape and species evolution: a look into the past. In: Hoorn C, Wesselingh FP, editors. The origin of the modern Amazon rainforest: implications of the palynological and palaeobotanical record. Oxford: Blackwell. p. 317–334.
Jurka J, Bao W, Kojima KK. 2011. Families of transposable elements, population structure and the origin of species. Biol Direct. 6(1):44.
Jurka J, Bao W, Kojima KK, Kohany O, Yurka MG. 2012. Distinct groups of repetitive families preserved in mammals correspond to different periods of regulatory innovations in vertebrates. Biol Direct. 7(1):36.
Jurka J, et al. 2005. Repbase Update, a database of eukaryotic repetitive elements. Cytogenet Genome Res. 110(1–4):462–467.
Kajikawa M, Okada N. 2002. LINEs mobilize SINEs in the eel through a shared 3′ sequence. Cell 111(3):433–444.
Kapusta A, Suh A. 2017. Evolution of bird genomes-a transposon's-eye view. Ann NY Acad Sci. 1389(1):164–185.
Kapusta A, Suh A, Feschotte C. 2017. Dynamics of genome size evolution in birds and mammals. Proc Natl Acad Sci U S A. 114(8):E1460–E1469.
Kazazian HH Jr. 2004. Mobile elements: drivers of genome evolution. Science 303(5664):1626–1632.
Kidwell MG, Lisch D. 1997. Transposable elements as sources of variation in animals and plants. Proc Natl Acad Sci U S A. 94(15):7704–7711.
Kohany O, Gentles AJ, Hankus L, Jurka J. 2006. Annotation, submission and screening of repetitive elements in Repbase: Repbasesubmitter and Censor. BMC Bioinformatics 7(1):474.
Koonin EV. 2016a. Horizontal gene transfer: essentiality and evolvability in prokaryotes, and roles in evolutionary transitions. F1000Res. 5:1805.
Koonin EV. 2016b. Viruses and mobile elements as drivers of evolutionary transitions. Philos Trans R Soc Lond B Biol Sci. 371. (https://doi.org/10.1098/rstb.2015.0442)
Kozak KM, et al. 2015. Multilocus species trees show the recent adaptive radiation of the mimetic *Heliconius* butterflies. Syst Biol. 64(3):505–524.
Kronforst MR. 2008. Gene flow persists millions of years after speciation in *Heliconius* butterflies. BMC Evol Biol. 8(1):98.
Kumar S, Stecher G, Suleski M, Hedges SB. 2017. TimeTree: a resource for timelines, timetrees, and divergence times. Mol Biol Evol. 34(7):1812–1819.
Kumar S, Stecher G, Tamura K. 2016. MEGA7: molecular evolutionary genetics analysis version 7.0 for bigger datasets. Mol Biol Evol. 33(7):1870–1874.
Lamichhaney S, et al. 2015. Evolution of Darwin's finches and their beaks revealed by genome sequencing. Nature 518(7539):371.
Lander ES, et al. 2001. Initial sequencing and analysis of the human genome. Nature 409(6822):860–921.
Lavoie CA, Platt RN, Novick PA, Counterman BA, Ray DA. 2013. Transposable element evolution in *Heliconius* suggests genome diversity within Lepidoptera. Mob DNA. 4:21.
Levy O, Knisbacher BA, Levanon EY, Havlin S. 2017. Integrating networks and comparative genomics reveals retroelement proliferation dynamics in hominid genomes. Sci Adv. 3(10):e1701256.
Lewis JJ, Reed RD. 2018. Genome-wide regulatory adaptation shapes population-level genomic landscapes in *Heliconius*. Mol Biol Evol. 36(1):159–173.
Li H. 2013. Aligning sequence reads, clone sequences and assembly contigs with BWA-MEM. arXiv. doi: doi: arXiv: 1303.3997. (https://arxiv.org/abs/1303.3997), and to the github repository (https://github.com/lh3/bwa).
Li H, Durbin R. 2011. Inference of human population history from individual whole-genome sequences. Nature 475(7357):493–484.
Li H, et al. 2009. The Sequence Alignment/Map format and SAMtools. Bioinformatics 25(16):2078–2079.
Li WZ, Godzik A. 2006. Cd-hit: a fast program for clustering and comparing large sets of protein or nucleotide sequences. Bioinformatics 22(13):1658–1659.
Lim JK, Simmons MJ. 1994. Gross chromosome rearrangements mediated by transposable elements in *Drosophila melanogaster*. Bioessays 16(4):269–275.
Lu J, Clark AG. 2010. Population dynamics of PIWI-interacting RNAs (piRNAs) and their targets in *Drosophila*. Genome Res. 20(2):212–227.
Martin M. 2011. Cutadapt removes adapter sequences from high-throughput sequencing reads. Embnet J. 17(1):10.
Martin SH, et al. 2016. Natural selection and genetic diversity in the butterfly *Heliconius melpomene*. Genetics 203(1):525.
Mavarez J, et al. 2006. Speciation by hybridization in *Heliconius* butterflies. Nature 441:868–871.
McClintock B. 1956. Controlling elements and the gene. Cold Spring Harb Symp Quant Biol. 21:197–216.
McClintock B. 1984. The significance of responses of the genome to challenge. Science 226(4676):792–801.
McKenna A, et al. 2010. The Genome Analysis Toolkit: a MapReduce framework for analyzing next-generation DNA sequencing data. Genome Res. 20(9):1297–1303.
Mita P, Boeke JD. 2016. How retrotransposons shape genome regulation. Curr Opin Genet Dev. 37:90–100.

Nadeau NJ, et al. 2012. Genomic islands of divergence in hybridizing *Heliconius* butterflies identified by large-scale targeted sequencing. Phil Trans R Soc B. 367(1587):343–353.
Nater A, Burri R, Kawakami T, Smeds L, Ellegren H. 2015. Resolving evolutionary relationships in closely related species with whole-genome sequencing data. Syst Biol. 64(6):1000–1017.
Ohshima K, Okada N. 2005. SINEs and LINEs: symbionts of eukaryotic genomes with a common tail. Cytogenet Genome Res. 110(1–4):475–490.
Oliver KR, Greene WK. 2011. Mobile DNA and the TE-Thrust hypothesis: supporting evidence from the primates. Mob DNA. 2(1):8.
Oliver KR, Greene WK. 2012. Transposable elements and viruses as factors in adaptation and evolution: an expansion and strengthening of the TE-Thrust hypothesis. Ecol Evol. 2(11):2912–2933.
Pasquesi GIM, et al. 2018. Squamate reptiles challenge paradigms of genomic repeat element evolution set by birds and mammals. Nat Commun. 9(1):2774.
Peccoud J, Loiseau V, Cordaux R, Gilbert C. 2017. Massive horizontal transfer of transposable elements in insects. Proc Natl Acad Sci U S A. 114(18):4721–4726.
Petrov DA, Schutzman JL, Hartl DL, Lozovskaya ER. 1995. Diverse transposable elements are mobilized in hybrid dysgenesis in *Drosophila virilis*. Proc Natl Acad Sci U S A. 92(17):8050–8054.
Platt RN 2nd, Blanco-Berdugo L, Ray DA. 2016. Accurate transposable element annotation is vital when analyzing new genome assemblies. Genome Biol Evol. 8(2):403–410.
Rebollo R, Horard B, Hubert B, Vieira C. 2010. Jumping genes and epigenetics: towards new species. Gene 454(1–2):1–7.
Rebollo R, Romanish MT, Mager DL. 2012. Transposable elements: an abundant and natural source of regulatory sequences for host genes. Annu Rev Genet. 46 46:21–42.
Reichardt J, Bornholdt S. 2006. Statistical mechanics of community detection. Phys Rev E Stat Nonlin Soft Matter Phys. 74(1 Pt 2):016110.
RepeatMasker [Internet]. 2013–2015. Available from: http://repeatmasker.org.
RepeatModeler Open-1.0 [Internet]. 2008–2010. Available from: http://www.repeatmasker.org.
Rey O, Danchin E, Mirouze M, Loot C, Blanchet S. 2016. Adaptation to global change: a transposable element-epigenetics perspective. Trends Ecol Evol. 31(7):514–526.
Rice P, Longden I, Bleasby A. 2000. EMBOSS: the European molecular biology open software suite. Trends Genet. 16(6):276–277.
Roy-Engel AM, et al. 2002. Active *Alu* element "A-tails": size does matter. Genome Res. 12(9):1333–1344.
Rull V. 2011. Neotropical biodiversity: timing and potential drivers. Trends Ecol Evol. 26(10):508–513.
Smit AFA, Hubley, R & Green, P. RepeatMasker Open-4.0. 2013–2015 <http://www.repeatmasker.org>.
Smit AFA, Hubley, R. RepeatModeler Open-1.0. 2008–2015 <http://www.repeatmasker.org>.
Sookdeo A, Hepp CM, Boissinot S. 2018. Contrasted patterns of evolution of the LINE-1 retrotransposon in perissodactyls: the history of a LINE-1 extinction. Mob DNA. 9.
Sundaram V, et al. 2014. Widespread contribution of transposable elements to the innovation of gene regulatory networks. Genome Res. 24(12):1963–1976.
Sundaram V, et al. 2017. Functional cis-regulatory modules encoded by mouse-specific endogenous retrovirus. Nat Commun. 8(1).
Supple M, Papa R, Counterman B, McMillan WO. 2014. The genomics of an adaptive radiation: insights across the Heliconius Speciation Continuum. Ecol Genomics Ecol Evol Genes Genomes 781:249–271.
Supple MA, et al. 2013. Genomic architecture of adaptive color pattern divergence and convergence in *Heliconius* butterflies. Genome Res. 23(8):1248–1257.
Talla V, et al. 2017. Rapid increase in genome size as a consequence of transposable element hyperactivity in wood-white (Leptidea) butterflies. Genome Biol Evol. 9(10):2491–2505.
Tarasov A, Vilella AJ, Cuppen E, Nijman IJ, Prins P. 2015. Sambamba: fast processing of NGS alignment formats. Bioinformatics 31(12):2032–2034.
Trizzino M, et al. 2017. Transposable elements are the primary source of novelty in primate gene regulation. Genome Res. 27(10):1623–1633.
Wang W, Kirkness EF. 2005. Short interspersed elements (SINEs) are a major source of canine genomic diversity. Genome Res. 15(12):1798–1808.
Waterston RH, et al. 2002. Initial sequencing and comparative analysis of the mouse genome. Nature 420(6915):520–562.
Yang L, Scott L, Wichman HA. 2019. Tracing the history of LINE and SINE extinction in sigmodontine rodents. Mob DNA. 10.
Zeh DW, Zeh JA, Ishida Y. 2009. Transposable elements and an epigenetic basis for punctuated equilibria. Bioessays 31(7):715.

Associate editor: Sarah Schaack